Arabian Journal for Science and Engineering
https://doi.org/10.1007/s13369-024-09127-x

RESEARCH ARTICLE-MECHANICAL ENGINEERING

Heat Transfer Augmentation in Thermally Enhanced Square Duct with Different Working Fluids

Hrishiraj Ranjan[1]

Received: 11 December 2023 / Accepted: 25 April 2024

Abstract
The improvement in the efficiency of the thermal system can be achieved by disrupting the laminar flow of fluid and boundary layer separators. Passive techniques are already incorporated by industries because it increases heat transfer rate up to many folds. The numerical investigation purpose is to find techniques for heat transfer augmentation in the square duct in the laminar flow regime. The thermo-hydraulic characteristics of ribs and helical screw tape (HST) insert fitted in the square ducts have been presented. The effect of rib orientations on the Nusselt number has been analyzed by the Finite volume-based commercial software ANSYS "Fluent". A SIMPLE algorithm has been used. The fluids having different Prandtl numbers are investigated under an imposed uniform wall heat flux boundary condition. The combination performance is better than the bare and ribbed square ducts. The 45° angled ribs with HST performance is better than the combination of transverse ribs with HST. At Reynolds number 200, the Nusselt number achieved by 45° angled ribs with HST is 4.3% higher than the 30° angled ribs with HST, 22.26% higher than the 60° angled ribs, and 35.82% higher than the transverse ribs with HST. Among the three working fluids, the Nusselt number for Servo-therm oil is the highest because Servo-therm oil minimizes entropy generation. Also, the thermal enhancement factor is greater than one for all considered cases and it is the highest for Servo-therm oil is the highest.

Keywords Ribs · Helical screw tape inset · Laminar flow regime · Entropy generation analysis · Thermal enhancement factor · Heat transfer augmentation · Thermo-hydraulic characteristics

List of Symbols

A	Heat transfer area (m^2)
L	Length of testing section (m)
AR	Aspect ratio
d	Rod diameter for helical screw tape (mm)
D_h	Hydraulic diameter of the test section (mm)
Δp	Pressure drop between entry and exit (Pa)
H	Pitch of the tape for 180° rotation
p	WD_h/d Screw tape parameter (mm)
P	Rib pitch (mm)
e	Rib height (mm)
W	Transverse distance covered by screw tape insert upon completing a pitch (mm)

Greek Symbols

δ	Tape thickness (mm)
ρ	Density of the fluid (kg/m^3)
μ	Fluid dynamic viscosity (kg/m s)

Non-dimensional Numbers

f	Friction factor of augmented square duct
f	Friction factor of bare square duct
Gz	Graetz number (dimensionless)
Nu	Nusselt number of augmented square duct
Nu_o	Nusselt number of bare square duct
TEF	Thermal enhancement factor
Pr	Prandtl number
U, V, W	Non-dimensional values of flow velocities (u, v, w) in Cartesian coordinate system, $U = {}^{u}/_{\overline{w}}$, $V = {}^{v}/_{\overline{w}}$, $W = {}^{w}/_{\overline{w}}$
P/e	Rib pitch

✉ Hrishiraj Ranjan
hrishi.ssec@gmail.com

[1] Mechanical Engineering Department, IIEST Shibpur, Howrah, West Bengal 711103, India

Published online: 27 May 2024

1 Introduction

The researchers of the modern era know that energy sources are limited, and we have to use them wisely. Energy conservation and conversion of unutilized energy are the future of thermal science. Over the past 40 years, heat exchangers have been extensively investigated (Both numerically and experimentally). The outcomes of the research are already incorporated into different types of industrial heat exchangers. Typically, heat exchangers are used in most industries like automotive, aviation, agricultural, dairy, process, etc. The heat exchangers are used to increase the heat transfer between two media [1].

Based on contact between working media, Heat Exchangers are of two types, Direct contact (Recuperators) and indirect contact (Regenerators) [2]. Technically, heat exchangers are used for energy conservation, conversion, and recovery of unutilized energy. The thermal and mechanical design of any heat exchanger depends on the application and availability of space. In industries, typically, circular, rectangular, and hexagonal-shaped ducts and pipes are used. The combination of transverse ribs with helical screw tape inserts in the square duct has been numerically investigated in this research work.

More often than not, water is used as a working fluid in heat exchangers. The flow regime (Laminar, Turbulent, and Transition) of the working fluid depends on application and conditions. A large number of engineering applications are based on the laminar flow regime because the laminar flow is predictable. In this research problem, the flow regime is the laminar flow regime.

The heat transfer enhancement techniques are more useful in the laminar flow regime because of the development of the thicker thermal boundary adjacent to the wall. The higher thermal resistance tends to minimize the heat transfer rate and this becomes more severe with viscous fluids. There are many passive techniques used for reducing thermal resistance like wire coil, ribs, surface roughness, dimpled tube, etc. [3, 4]. Regularly spaced transverse ribs have been used in this problem. Also, at the core of fluid flow, there is no proper mixing of the fluid. The particles follow streamlines. This generates thermal resistance and thus, the rate of heat transfer decreases. A helical screw tape insert is placed at the center of the square duct. This insert will provide better mixing and increase the rate of heat transfer [5].

There are a large number of research available in open literature where the combination of two passive heat transfer enhancement techniques was used. Sivashanmugam and Suresh [6] experimented with regularly spaced helical screw tape inserts in a circular tube and presented the heat transfer and friction factor characteristics. They observed a decrease in Nusselt number of about 10% and about 5% in friction factor for every 100 mm increase in spacer length. Also, an increase in the twist ratio adversely affects the Nusselt number. They presented empirical correlations for both laminar flow and turbulent flow regimes. Rout and Saha [7] experimentally investigated heat transfer and pressure drop characteristics of laminar flow through a circular tube fitted with two passive heat transfer enhancement techniques, wire-coil, and helical-screw tape inserts. They found an increment of 45–78% in heat transfer for constant pumping power. also, a significant 35–55% reduction in pumping power for constant heat duty has been observed. Based on performance evaluation, they claimed that the performance of the combination of passive heat transfer enhancement techniques is better than of a single passive heat transfer enhancement technique and bare tube. They generated a correlation for the Nusselt number and f Re which is based on log-linear regression analysis. Ranjan et al. [8] presented the results of different combinations of passive heat transfer enhancement techniques in non-circular channels in the laminar flow domain regime. This investigation covered a wide range of Prandtl numbers. They claimed that there is a 31–52% increase in heat duty at constant pumping power and a 25–36% reduction in pumping power at constant heat duty. Chaurasia and Sarviya [9] numerically and experimentally studied the thermo-hydraulic performance of helical screw tape insert in a circular tube in a transition flow regime. They compared three twist ratios (1.5, 2.5, and 3) and discussed the effect of the single-strip and double-strip helical screw tape inserts on the Nusselt number and friction factor. Also, there is an increase in the Nusselt number with a decrease in the twist ratio. They achieved a maximum heat transfer enhancement of 2.82 times that of the bare tube. Ranjan and Saha [10] numerically investigated the transverse ribs and helical screw tape inserts in the non-circular duct. Ribs are mounted on four walls and they observed the heat transfer augmentation. They compared five different liquids and presented a performance data evaluation table.

Han and Park [11] experimentally investigated rib turbulators fitted with square channels in the turbulent flow regime. Ribs were mounted on the two opposite sides of the rectangular duct. They examined the rib angle-of-attack and found the highest heat transfer and pressure drop for $\alpha = 60°$ in the square channel. Also, they observed that the angled rib heat transfer performance is about 30% higher than the transverse ribs fitted for the square channel at a constant pumping power. They presented empirical correlations for heat transfer and friction factors. Similarly, Promvonge et al. [12] numerically investigated the heat transfer and friction factor characteristics in a square duct fitted with 45° inline baffles on two opposite walls. Typically, researchers used single passive heat transfer enhancement techniques but some researchers used compound heat transfer enhancement techniques. Saha et al. [13] examined axial corrugations and fitted them with helical screw-tape inserts in a circular tube in a laminar flow regime. Similarly, Saha and Saha [14] used integral helical rib

roughness with helical screw tape inserts in a circular tube. Moon et al. [15] numerically investigated different rib shapes in the rectangular channel and proposed the new boot-shaped design rib performance is the best among all. Similarly, Keklikcioglu and Ozceyhan [16] published a review report on compound heat transfer enhancement techniques where they focused on Wire coil inert and twisted tape Inserts. Sharma et al. [17] experimentally investigated the pentagonal ribs in the rectangular duct at Reynolds number ranging from 9400 to 58,850. They observed heat transfer augmentation at a low heat transfer zone. The above-mentioned research ideas are emphatic but there are not enough research ideas incorporating the compound heat transfer enhancement techniques in square channels. In this research, transverse ribs are fitted on the opposite walls of the square duct and a helical screw tape insert is positioned in the center of the square duct. The thermo-hydraulic characteristics of the compound heat transfer enhancement techniques have been presented.

Also, modeling of non-Newtonian fluids in the case of heat generation and absorption plays an important role in heat transfer. Ali et al. [18], Ali et al. [19] and Rehman et al. [20] examined numerically the flow field and temperature characteristics of Carreau fluid around a wedge and in a thermally stratified medium. Similarly, Rehman et al. [21] investigated the heat transfer characteristics of Williamson fluid under the imposed magnetic field and found that Williamson fluid velocity decreases with an increase in magnetic field parameters. Bibi et al. [22] worked with two-dimensional unsteady solid-particle flow having variable thermal conductivity. They found that the Nusselt number decreases significantly with a collective increase in parameters like thermal conductivity and power-law index. Acharya and Oztop [23] investigated the hydrothermal characteristics of magnetically driven buoyancy-induced hybrid nanofluids (Al_2O_3-TiO_2-water) through a semi-circular chamber having a different aspect ratio of triangular size heater at the bottom. They discussed the effect of aspect ratio on u and v velocity. Similarly, Acharya [24] examined the hydrothermal behavior of buoyancy-driven multi-walled carbon nanotube (MWCNT)-Fe3O4-Water hybrid nanofluid equipped with T-shaped fins. He discussed different cases and concluded that Rayleigh number assist buoyancy-driven motion.

Although, a large number of published research work based upon laminar flow is available in open literature, but introduction of combined heat transfer enhancement techniques in square duct in laminar flow regime has not been numerically investigated. The Industries have incorporated rib turbulators in circular tubes for a long time ago, but according to requirement and space constraints, square ducts could be incorporated in different industries. The major advantage of the square channel is that the ribs can be easily and precisely installed at respective positions. The above-proposed combination in a square duct is new to all. The effect of rib angles in the presence of HST, reduces the boundary layer thickness effectively and provides effective mixing of the working fluid. The novelty in the study is the bulk fluid mixing and effective reduction in boundary layer thickness with the combined passive heat transfer enhancement techniques in a square duct. Also, the fluid particle motions at different cross sections have been presented which enables a researcher to visualize the effect of ribs and HST working in tandem. Additionally, the use of different working fluids facilitates us to know the effect of combined techniques on thermal diffusivity and momentum diffusivity. This study is important for transportation of viscous fluids, highly flammable fluids through pipes/ducts where heat dissipation is more important than loss in pressure. The heat transfer enhancement techniques are known to most thermal science professionals and are not new, nevertheless, industries-oriented positioning and placement of heat transfer techniques always have novelty.

2 Mathematical Modeling

The advancement in computational power and availability of high-end computers are making numerical analysis more useful in the thermal field. Nowadays, commercially packaged solvers are frequently used in research work because it is accurate, save time, are cost-effective, and are reliable. ANSYS Fluent has been used for solving the above-mentioned problem because it works on Finite Volume Method. The FVM is a discretization technique. The beauty of FVM is that the numerical flux is locally conserved at each cell and each cell (Control volume) follows local balance. Thus, FVMs are frequently used in Aerospace engineering, fluid engineering and heat, and mass transfer [25].

2.1 Problem Description

The square duct fitted with ribs and HST is designed in ANSYS Design Modeler. The heat transfer and pressure drop calculations are the objective of the present study, thus, only the fluid domain has been created in Design Modeller. This idea reduces the number of elements in meshing and reduces elapsed time.

The combination of two passive heat transfer enhancement techniques, transverse ribs with helical screw tape (HST) inserts in a square duct has been presented in Fig. 1a. Similarly, the angled ribs with HST inserts in a square duct has been shown in Fig. 1b.

The flow is in a positive z-direction. The transverse ribs are mounted on the two opposite walls of the square duct. The helical screw tape insert is placed at the center of the square duct. The configuration of the angled ribs is the same

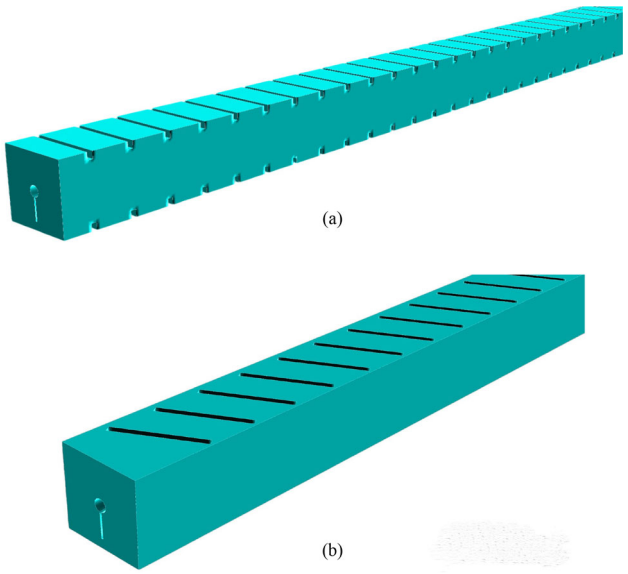

Fig. 1 **a** Transverse ribs in combination with HST fitted in a square duct, and **b** Angled ribs in combination with HST fitted in a square duct

as shown in Fig. 1, except the inclination of ribs. The angle has been measured from the flow direction of the fluid.

Additionally, the geometrical parameters are presented in the Fig. 2. The green-colored geometries are representing the inserts used.

The hydraulic diameter ($D_h = 4A_c/P_W$) of the square duct is 13 mm and length to diameter ratio (L/D_h) is 70. A_c denotes cross-sectional area and P_w denotes wetted perimeter. The non-dimensional rib height (e/D_h) is 0.1026 and the non-dimensional rib pitch (P/e) is 5.6481. e denotes the rib height. The helical screw tape pitch is defined as $p = WD_h/d$ where W is the transverse distance covered by screw tape insert upon completing a pitch, mm. The helical screw tape pitch insert is 52 mm. The core rod diameter d is 2 mm. The helical screw tape thickness δ is 0.5 mm.

2.2 Problem Formulation

In the internal flow conditions, the heat transfer rate can be increased by either increasing the flow rate or by decreasing the boundary layer thermal resistance. Surface roughness, ribs, and wire coils may be used but, in this investigation, transverse ribs and angled ribs are mounted on the opposite side of the walls of the square duct. Typically, the manufacturing process of transverse ribs is easy and economical. Also, bulk mixing is generally provided by twisted tape, screw tape, vortex generator, etc. Out of these, a Helical screw tape insert with a center rod is used and it is positioned at the center of the duct. The thermo-hydraulic characteristics of different fluids should be different. The research aims to know the thermal performance of different working fluids.

Three working fluids are Water (Pr = 5.89), Ethylene Glycol (Pr = 150.45), and Servo-therm oil (Pr = 443.117). The properties have been presented in Table 1

The following assumptions are imposed on the numerical model. This assumption decreases the computation time without affecting the accuracy.

- The working fluid is incompressible.
- Laminar flow regime, Steady-state fluid flow and heat transfer
- Fluid properties are constant except viscosity.
- Body forces and viscous dissipation are ignored.
- Heat flux is directly applied to the working fluids.
- The helical screw tape wall is adiabatic.
- The Duct surface is smooth and the walls are impermeable.

2.3 Governing Equations

The fluid dynamics is based on three fundamental physical principles "Mass Conservation, Newton's second law and energy conservation". The mathematical statement for the fluid flow and heat transfer problem are Continuity equation, momentum equation, and energy equation [29].

Continuity equation:

$$\nabla(\rho \vec{V}) + \frac{\partial \rho}{\partial t} = 0 \tag{1}$$

Since the fluid is in a steady-state condition. So, the applied continuity equation will be

$$\nabla(\rho \vec{V}) = 0 \text{ or } \rho\left(\frac{\partial u_x}{\partial x} + \frac{\partial u_y}{\partial y} + \frac{\partial u_z}{\partial z}\right) = 0 \tag{2}$$

Navier stoke equation

$$\frac{\partial}{\partial t}(\rho u_i) + \frac{\partial}{\partial x_j}(\rho u_i u_j) = -\frac{\partial p}{\partial x_i} + \frac{\partial}{\partial x_j}\left(\mu \frac{\partial u_i}{\partial x_j}\right) + \frac{\partial}{\partial x_i}\left[(\lambda + \mu)\frac{\partial u_k}{\partial x_k}\right] + \rho b_i \tag{3}$$

On imposing above mentioned assumption and considering mechanical pressure is equal to thermodynamic pressure, the momentum equation is reduced as

$$\rho\left(u\frac{\partial u}{\partial x} + v\frac{\partial u}{\partial y} + w\frac{\partial u}{\partial z}\right) = -\frac{\partial p}{\partial x} + \mu\left(\frac{\partial^2 u}{\partial x^2} + \frac{\partial^2 u}{\partial y^2} + \frac{\partial^2 u}{\partial z^2}\right) \tag{4}$$

$$\rho\left(u\frac{\partial v}{\partial x} + v\frac{\partial v}{\partial y} + w\frac{\partial v}{\partial z}\right) = -\frac{\partial p}{\partial y} + \mu\left(\frac{\partial^2 v}{\partial x^2} + \frac{\partial^2 v}{\partial y^2} + \frac{\partial^2 v}{\partial z^2}\right) \tag{5}$$

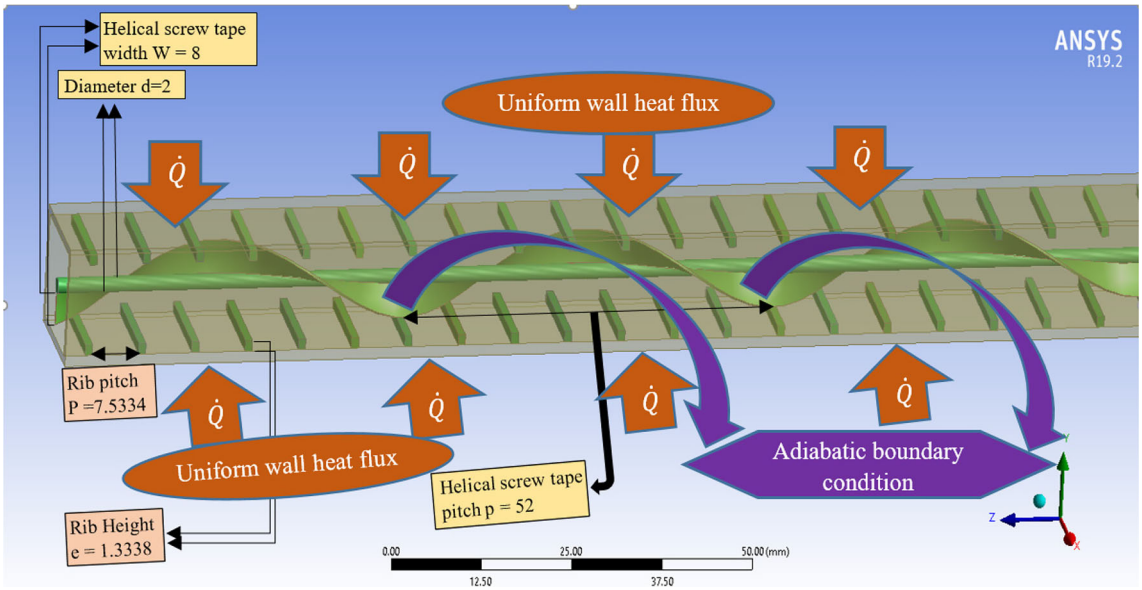

Fig. 2 The transverse ribs positioned on opposite faces and helical screw tape at the center of the square duct

Table 1 Working fluids and their properties

Working Fluids	Density (Kg/m^3)	Specific heat (KJ/kg K)	Thermal conductivity (W/m K)	Viscosity (Kg/m s)
Water [26]	996.59	4.179	0.606	0.000852
Ethylene glycol [27]	1111.4	2.415	0.252	0.0157
Servotherm oil [28]	805.386	1.768	0.1424	0.03569

$$\rho\left(u\frac{\partial w}{\partial x}+v\frac{\partial w}{\partial y}+w\frac{\partial w}{\partial z}\right)=-\frac{\partial p}{\partial z}+\mu\left(\frac{\partial^2 w}{\partial x^2}+\frac{\partial^2 w}{\partial y^2}+\frac{\partial^2 w}{\partial z^2}\right) \tag{6}$$

Energy equation

$$\left[u\frac{\partial T}{\partial x}+v\frac{\partial T}{\partial y}+w\frac{\partial T}{\partial Z}\right]=\alpha\left[\frac{\partial^2 T}{\partial x^2}+\frac{\partial^2 T}{\partial y^2}+\frac{\partial^2 T}{\partial z^2}\right] \tag{7}$$

2.4 Boundary Conditions

The flow regime is laminar and the Reynolds number is varying from 200 to 1000. At the inlet of the testing section, a fully developed velocity profile is introduced [30] and at the outlet section, the pressure outlet boundary condition is chosen means Gauge pressure = 0. The center point of duct is coinciding with origin and duct has been extruded along z-axis. In Cartesian co-ordinate system, under the steady laminar flow condition and applying boundary layer approximation, one can write the equation of motion as

$$U\frac{\partial W}{\partial X}+\alpha V\frac{\partial W}{\partial Y}+\frac{\alpha}{2\mathrm{Re}}W\frac{\partial W}{\partial Z^*}=\frac{\alpha}{4\mathrm{Re}}\frac{\mathrm{d}p^*}{\mathrm{d}z^*}+\frac{4}{(\alpha+1)\,\mathrm{Re}}\left[\frac{\partial^2 W}{\partial X^2}+\alpha^2\frac{\partial^2 W}{\partial Y^2}\right] \tag{8}$$

For uniform flow $W = 1$, and at the end of cross section $Z^* = Z_L^*$ and applying the boundary condition for incompressible flow, the equation for fully developed profile a square duct reduced as

$$W=\frac{3}{2}\left[\frac{\left\{1-Y^2-\frac{32}{\pi^3}\sum_{n=0}^{\infty}\frac{(-1)^n}{(2n+1)^3}\times\frac{\cosh(2n+1)\left(\frac{\pi}{2}\right)\alpha X}{\cosh(2n+1)\left(\frac{\pi}{2}\right)\alpha}\cos(2n+1)\frac{\pi}{2}Y\right\}}{\left\{1-\frac{192}{\pi^5\alpha}\sum_{n=0}^{\infty}\frac{1}{(2n+1)^5}\tanh(2n+1)\frac{\pi}{2}\alpha\right\}}\right] \tag{9}$$

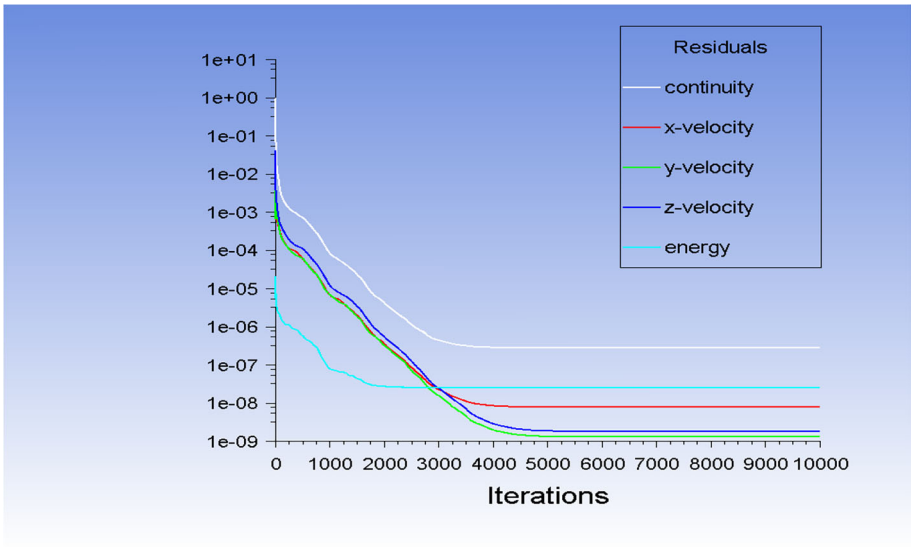

Fig. 3 Residual versus iterations for Re = 200 (Working Fluid: Water)

In CFD, the fully developed profile of any section can be found easily in two steps. First, take a bare geometry having same section and provide enough length so that flow become fully developed (Inlet velocity should be in laminar regime). Second step, the profile obtained at the outlet of bare geometry gives the fully developed profile. Copy the velocity profile and paste it at the inlet of the testing section.

Also, uniform wall heat flux has been imposed on the two opposite ribbed walls. The heat flux is directly introduced to the working fluid. The helical screw tape boundary wall is assumed to be adiabatic ($\dot{Q} = 0$) because no heat flux is applied to it. No slip boundary condition has been implemented over the channel walls as well as ribs and helical screw tape inserts.

3 Numerical Solution Approach

The Finite Volume Method based solver Fluent has been used to solve the equation [31]. The partial differential equations are discretized first and then the equations are solved by software-based programs. Although, there are four algorithms (SIMPLE, SIMPLEC, PISO, Fractional Step) in Fluent for Pressure–Velocity coupling but each of them has its own advantage. The semi-implicit pressure-linked equation (SIMPLE) algorithm [32] is best for steady state problems and it is a pressure-based solver. PISO and Fraction Step are used for transient problems. It should be noted that between the SIMPLEC and SIMPLE algorithm, the SIMPLE algorithm takes less computational time without affecting the results.

The Least Squares Cell-Based gradient is used to discretize the equation. Although, Point linear interpolation is also available for gradient discretisation, but it is used for irregular o bad mesh where it reduces skewness error. The Least Squares Cell-Based gradient method calculates the gradient in a cell which, when used to extrapolate the cell value to centers of all neighboring cells, minimizes the error between extrapolated values and cell values. This method perfectly supports SIMPLE scheme. The solution varies linearly. This is accurate on unstructured mesh too and it is less expensive. The second-order scheme for pressure, a second-order upwind scheme for momentum and a second-order upwind scheme has been used. The second-order schemes are better than standard and linear schemes but they may give poor results with bad mesh. The under-relaxation factors are 0.3 and 0.7 for pressure and momentum respectively. The solutions are assumed to converge when the equation achieves set residuals and values. The residuals vs iterations have been shown in Fig. 3. In Fig. 3, the ribs are mounted on the opposite walls whereas HST is placed at the center of the square duct. The working fluid is water and velocity at the inlet corresponds to Reynolds number 200. Although, for the above-mentioned case, residuals are of the order of 10^{-8}, as inlet velocity increases, the residuals are limited to the order of 10^{-7}. In CFD, the residuals should be as low as possible. Thus, an average value applicable for all cases is 10^{-6}, 10^{-7}, and 10^{-7} for continuity, velocity, and energy equations, which is good enough to get accurate results. As viscosity and velocity increase, it is very hard to get residuals below 10^{-7}. On average, a complete simulation takes 13–14 h.

4 Meshing

The numerical analysis credibility depends on the mesh quality. In this numerical investigation, the ANSYS Meshing Module has been used. The research problem geometry is

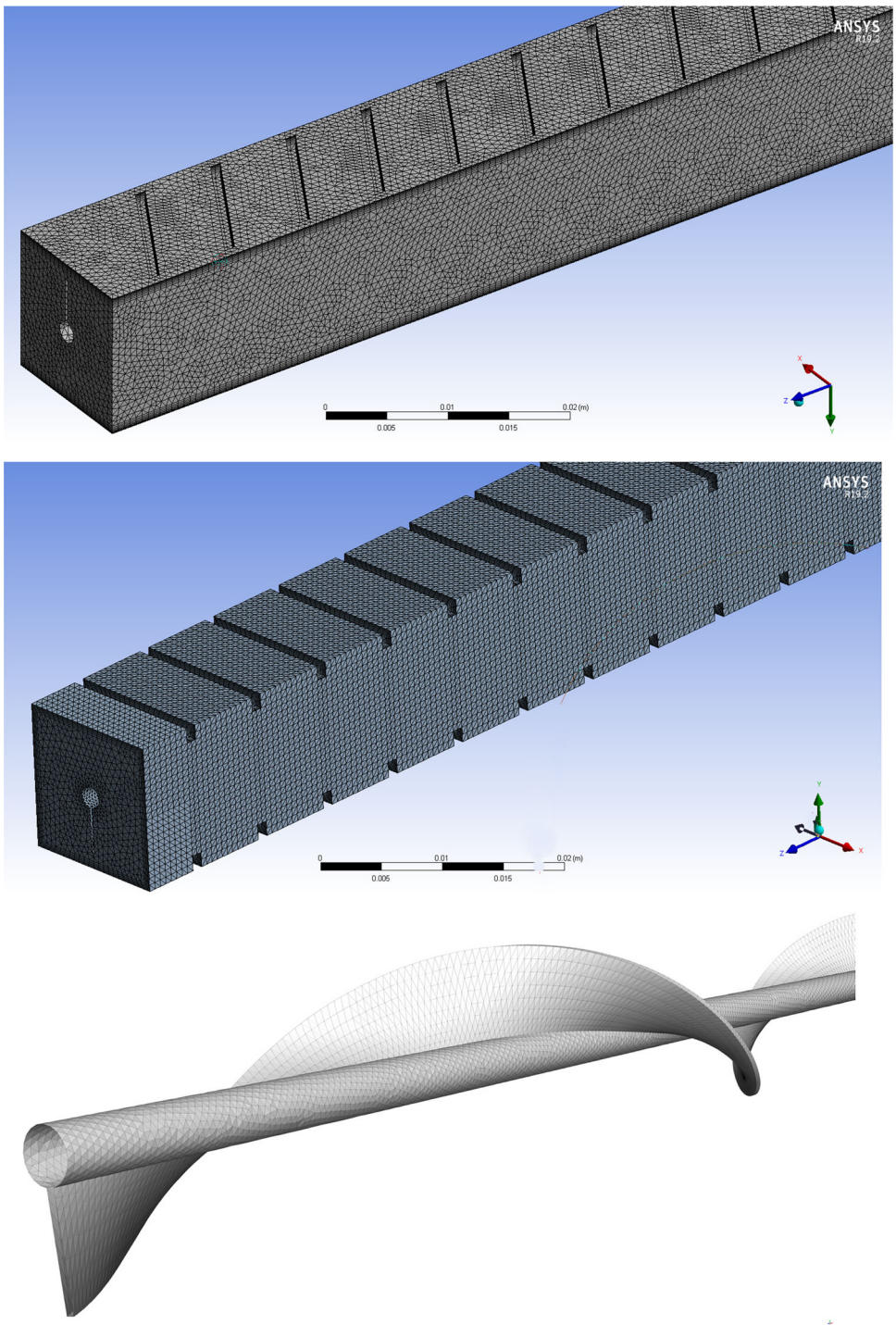

Fig. 4 Meshing of angled rib geometry, transverse rib geometry and only helical screw tape insert with center rod model

not symmetrical about any plane or axis. Thus, Regular automatic meshing, will not be able to handle this problem. Out of different methods, sizing, inflations, and face meshing are selected and imposed on the testing geometry. The meshing of the combination of passive heat transfer enhancement techniques is shown in Fig. 4.

The element size and number of inflation layers are decided by the Grid Independence test. Grid independence means that results do not depend on the meshing parameters. The grid independence test results are presented in Figs. 5 and 6. Two output parameters, the average total pressure at the outlet and the Nusselt number have been selected from a list of output parameters. In Fig. 5 average total pressure increases with an increase in the number of elements but after the element size 0.0006 m, the average. total pressure at the outlet became almost constant.

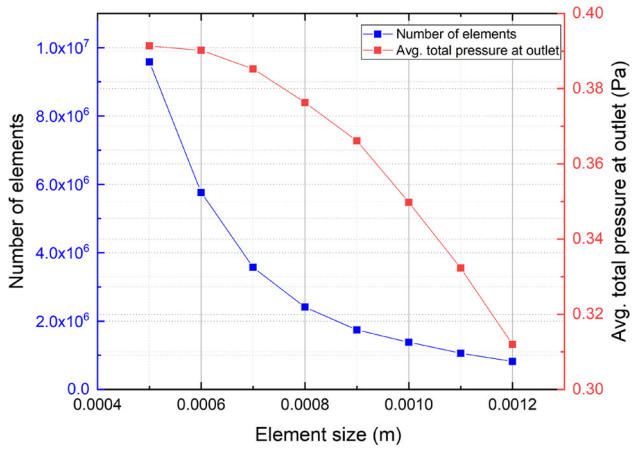

Fig. 5 Variation of average total pressure at outlet with element size

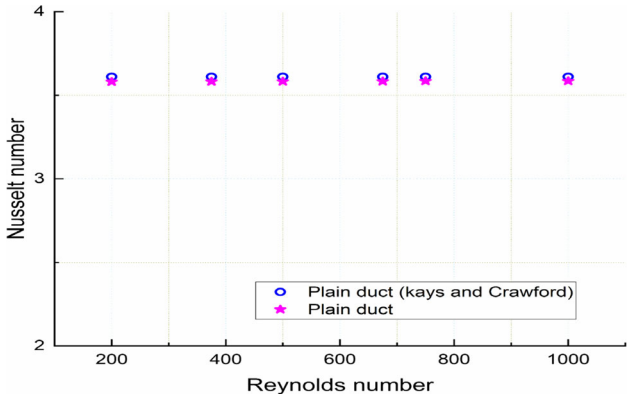

Fig. 7 Comparison of Nusselt number (numerically) with exact Nusselt number (experimentally and published) for the plain tube. (Kays and Crawford)

Similarly, the output parameter, Nusselt number decreases with the decrease in element size. After element size 0.0006 m, only a 0.02% change in the Nusselt number has been observed. From both graphs, we found the appropriate element size is 0.0006 m. Additionally, 5 layers of inflation and face meshing are imposed to reduce the maximum and average skewness of elements. The total number of elements is 5,760,737 at the element size of 0.0006 m. It should be noted that by further reducing the element size to 0.0005, there is an unacceptable increase in the number of elements 9,578,530 which will increase the simulation time up to many folds.

5 Validation with the Smooth Wall

The numerically investigated plain tube Nusselt number and friction factor (fRe) results are compared with the results available in the open literature for plain ducts. The results are in agreement with only a 0.9% error (Maximum) in the Nusselt number and only a 1.3% error in the fRe value (Maximum). The Nusselt number and friction factor for plain tube under uniform wall heat flux conditions [33]

$$\mathrm{Nu} = 3.61 \tag{10}$$

$$f\mathrm{Re} = 57 \tag{11}$$

Fig. 6 Variation of Nusselt number with element size

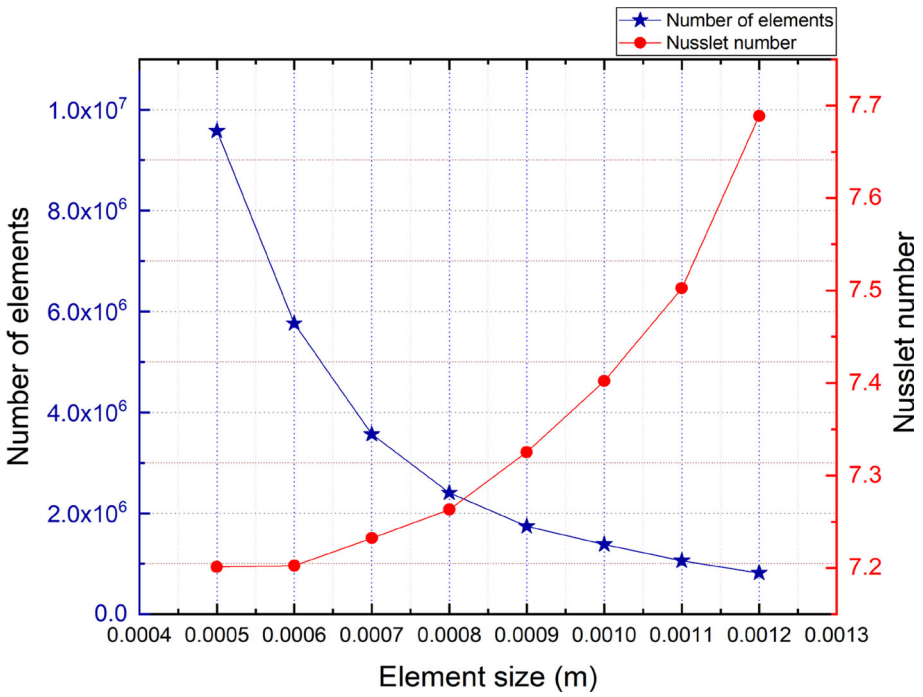

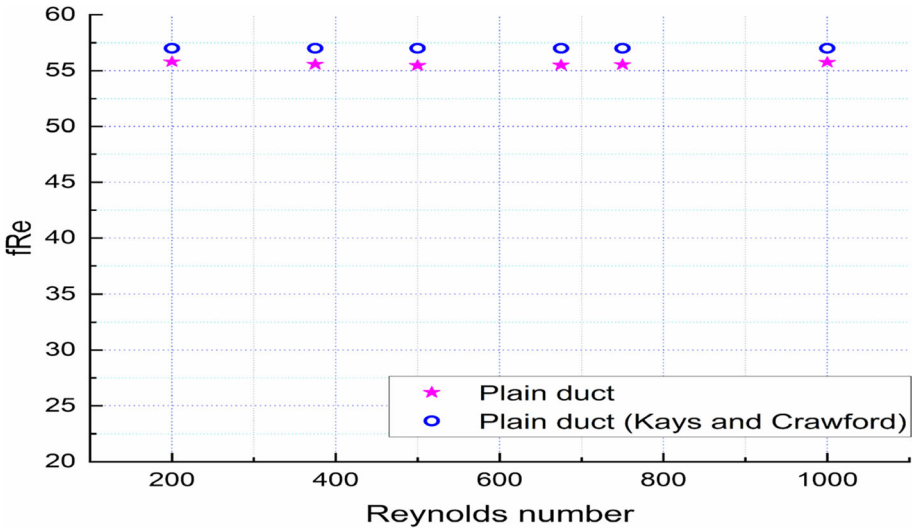

Fig. 8 Comparison of f Re value (numerically) with exact fRe value (experimentally and published) for plain tube. (Kays and Crawford)

This has been shown in Figs. 7 and 8. This research paper has reported the Nusselt number, friction factor, thermal performance, flow pattern, and heat transfer characteristics of the combination of passive techniques. The Reynolds number and Prandtl Number of fluid flowing in the duct are calculated by

$$\mathrm{Re} = \frac{\rho v D_\mathrm{h}}{\mu} \tag{12}$$

$$\mathrm{Pr} = \frac{\mu C_\mathrm{p}}{\kappa} \tag{13}$$

The Nusselt number is the ratio of convective heat transfer to conductive heat transfer and is expressed as

$$\mathrm{Nu} = {}^{hL}/_{k} \tag{14}$$

where

$$\dot{Q} = hA(T_\mathrm{w} - T_\mathrm{b}) \tag{15}$$

In the present problem, the numerical findings achieved by simulations are validated with the experimental data of Saha et al. [13]. They developed the correlations for the "Nusselt number" and "friction factor f" of a tube fitted with a "helical screw tape" insert and transverse ribs. The validation results are presented in Fig. 9. The empty symbols are results corresponding to experimental results presented by Saha et. al. [13] whereas the solid symbols are the results obtained by mathematical modeling and simulations. Both experimental and numerical results follow the same trend. The maximum discrepancy between experimental and numerical findings is nearly about fifteen percent [34].

The ribs and helical screw tape inserts are used in this research work. The inserts are blocking the free flow of working fluids, thus, a significant amount of pressure drop is observed. The Darcy friction factor has been calculated for all the considered cases and it is expressed as

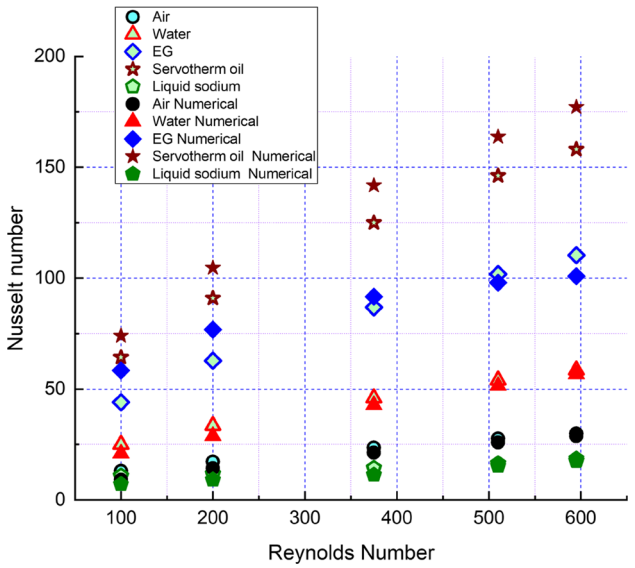

Fig. 9 The validation of numerical simulation results with the experimental results of Saha et. al. [13]

$$f = \frac{2\Delta p D_\mathrm{h}}{\rho L v^2} \tag{16}$$

The performance evaluation is essential in this case. There are many performance evaluation criteria but we are using "Thermal Enhancement Factor (TEF)" [35]. The thermal enhancement factor is the Nusselt number to friction factor

for thermally enhanced ducts to the bare duct. Mathematically, TEF is expressed as

$$\mathrm{TEF} = \frac{(\mathrm{Nu}/\mathrm{Nu}_o)}{(f/f_o)^{0.33}} \tag{17}$$

6 Entropy Generation Rate

Entropy is a measure of the disorder or randomness of a system. Entropy generation represents a loss of available energy, thus, it is important to minimize it. All the natural process increases the entropy of system. In this heat transfer problem, the application of compound heat transfer enhancement techniques can minimize entropy generation. The Eulerian approach has been adopted for heat transfer augmentation analysis. The approach for entropy generation analysis is, first we calculate entropy generation for a cell or infinitesimal control volume and integrate this for whole volume. The cells are obtained by meshing the domain. In FVM methods, the flux is locally conserved at the surface of cell. We can write the rate of entropy generation for an infinitesimal control volume as

$$\delta \dot{S}_{\mathrm{gen}} = \dot{m}\mathrm{d}s - \frac{\delta \dot{Q}}{T_{\mathrm{w}}} \tag{18}$$

where ds represent entropy change and $\delta \dot{Q}$ represent heat transfer rate transferred to fluid. Also,

$$\mathrm{d}s = \frac{C_{\mathrm{p}}\mathrm{d}T}{T} - \frac{\mathrm{d}P}{\rho T} \tag{19}$$

and

$$\delta \dot{Q} = \dot{m}C_p\mathrm{d}T = q''p\mathrm{d}x \tag{20}$$

where $q'' = \overline{h}(T_{\mathrm{w}} - T)$ is the heat flux and p is the perimeter. Substituting ds and $\delta \dot{Q}$, we get

$$\delta \dot{S}_{\mathrm{gen}} = \dot{m}C_{\mathrm{p}}\left(\frac{1}{T} - \frac{1}{T_{\mathrm{w}}}\right)\mathrm{d}T - \frac{\dot{m}}{\rho}\left(\frac{1}{T}\right)\mathrm{d}P \tag{21}$$

On doing mathematical substitutions and calculations, we get

$$\frac{\delta \dot{S}_{\mathrm{gen}}}{\dot{m}C_{\mathrm{p}}} = \left(\frac{1}{T} - \frac{1}{T_{\mathrm{w}}} + \frac{f\rho U^3}{8q''T}\right)\mathrm{d}T \tag{22}$$

where f is friction factor.

Considering the uniform wall heat flux boundary condition (q'' = constant) on the periphery of tube, we can write

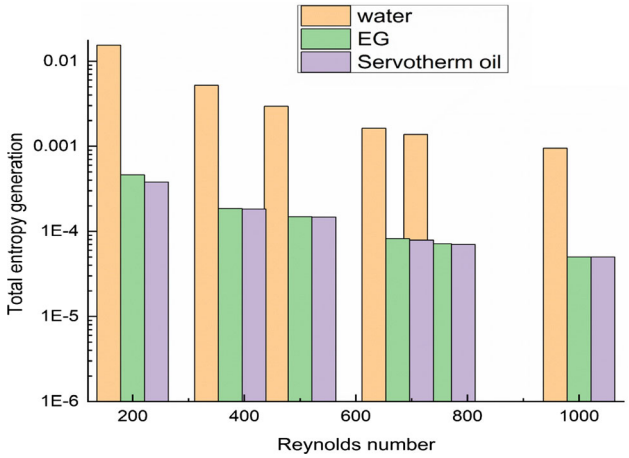

Fig. 10 Comparison of total entropy generation of water, ethylene glycol and servo-therm oil at different Reynolds number

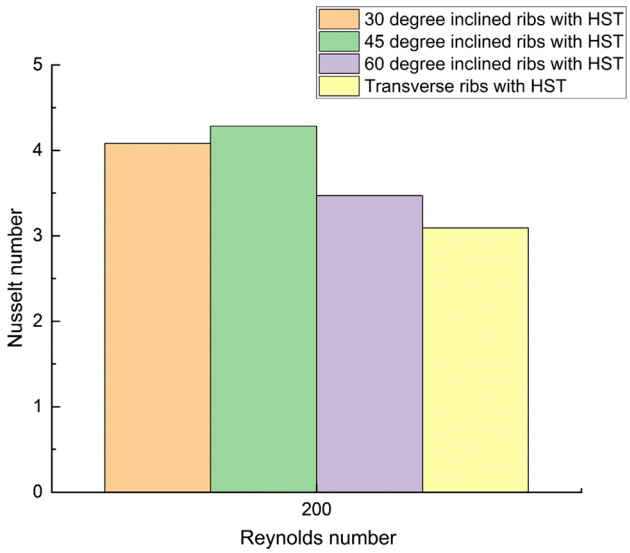

Fig. 11 Comparison of Nusselt number corresponds to ribs mounted at different angles in synergy with Helical screw tape inserts at Reynolds number 200

the

$$T_e = T_i + \frac{q''p}{\dot{m}C_p}L \tag{23}$$

On substituting proper conditions and doing some algebraic calculation, we obtained

$$\frac{\delta \dot{S}_{\mathrm{gen}}}{\dot{m}C_p} = \ln\left[\frac{(1+\theta)(1+\tau_q)}{1+\tau_q+\theta}\right] + F_q\ln(1+\theta) \tag{24}$$

where $\theta = \frac{T_e - T_i}{T_i} = \frac{q''pL}{\dot{m}C_{\mathrm{p}}T_i}$, $\tau_q = \frac{q''}{\bar{h}T_i}$ and $F_q = \frac{f\rho U^3}{8q''}$.

The above mention procedure has been implemented for 45° inclined ribs and helical screw tape insert fitted in square

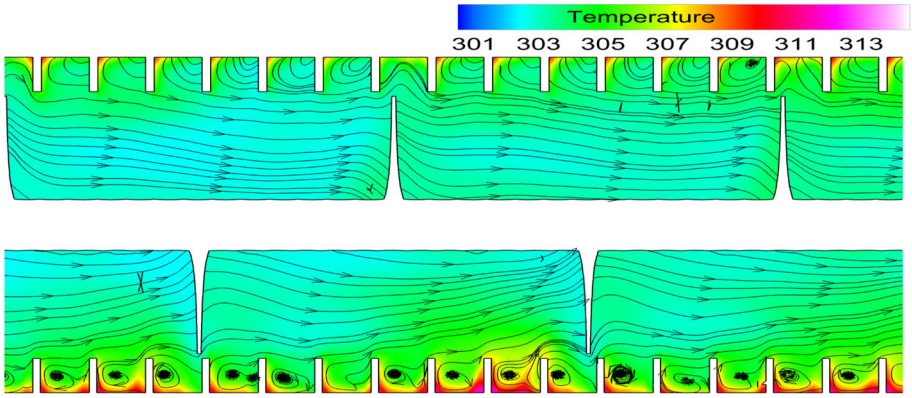

Fig. 12 Streamlines and temperature profile at Re = 500 for water (along the flow, cross-sectional view)

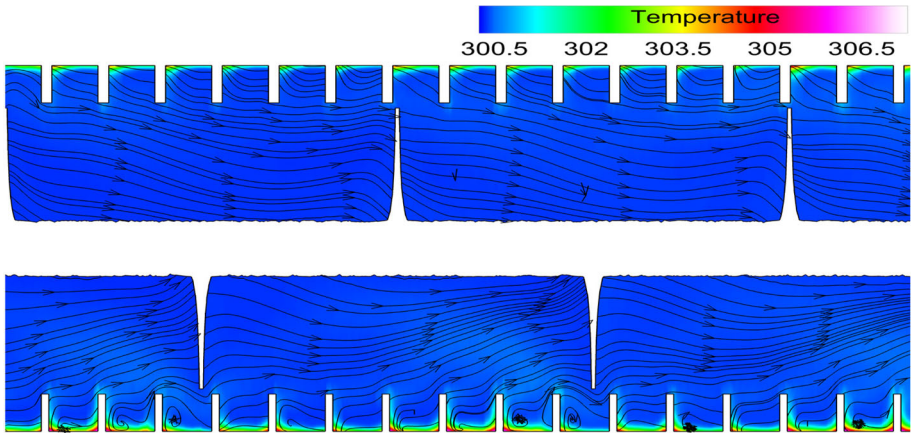

Fig. 13 Streamlines and temperature profile at Re = 500 for EG (along the flow, cross-sectional view)

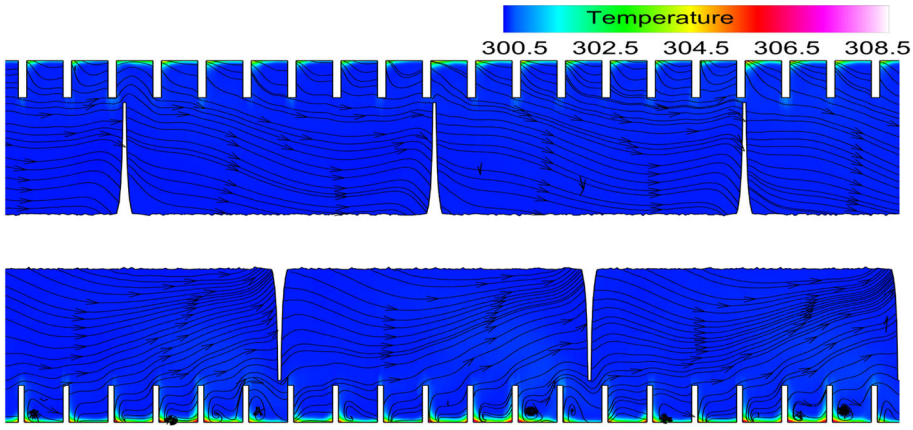

Fig. 14 Streamlines and temperature profile at Re = 500 for servo-therm oil (along the flow, cross-sectional view)

channel. The total entropy generation is shown in Fig. 10. The histogram shows that the working fluid water is generating more entropy than others. The total entropy generation for ethylene glycol is little higher than Servo-therm oil but at Reynolds number 1000, the entropy generated by both fluids are same. The viscosity of water is lower than the Ethylen glycol and Servo-therm oil. Considering the case of angled ribs with HST, the more the fluid is viscous, the more will be residence time because of direction toward heated wall. The high entropy generation means loss of efficiency. Thus, Ethylene glycol and Servo-therm oil are better than water in the laminar flow regime (Fig. 10).

7 Results and Discussion

The performance of angled ribs with HST and transverse ribs with HST have been compared. In both the arrangements, the helical screw tape with core rod is present at the axial location and ribs are fitted on opposite faces. Apart from transverse

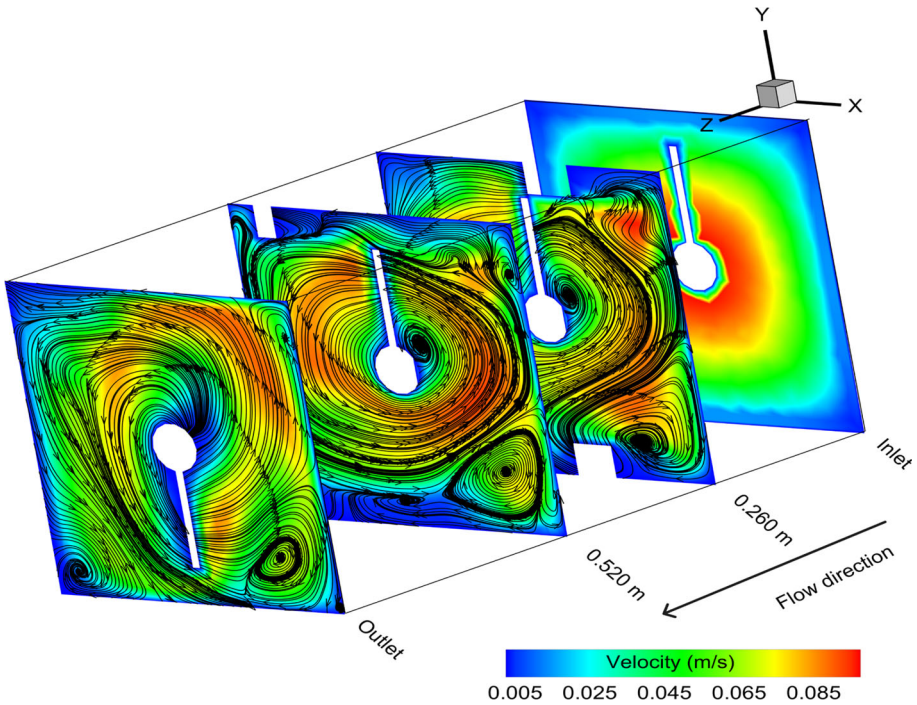

Fig. 15 Streamlines and velocity contours in a square duct fitted with 45° angled ribs on two opposite walls and HST, working fluid water at Re = 750

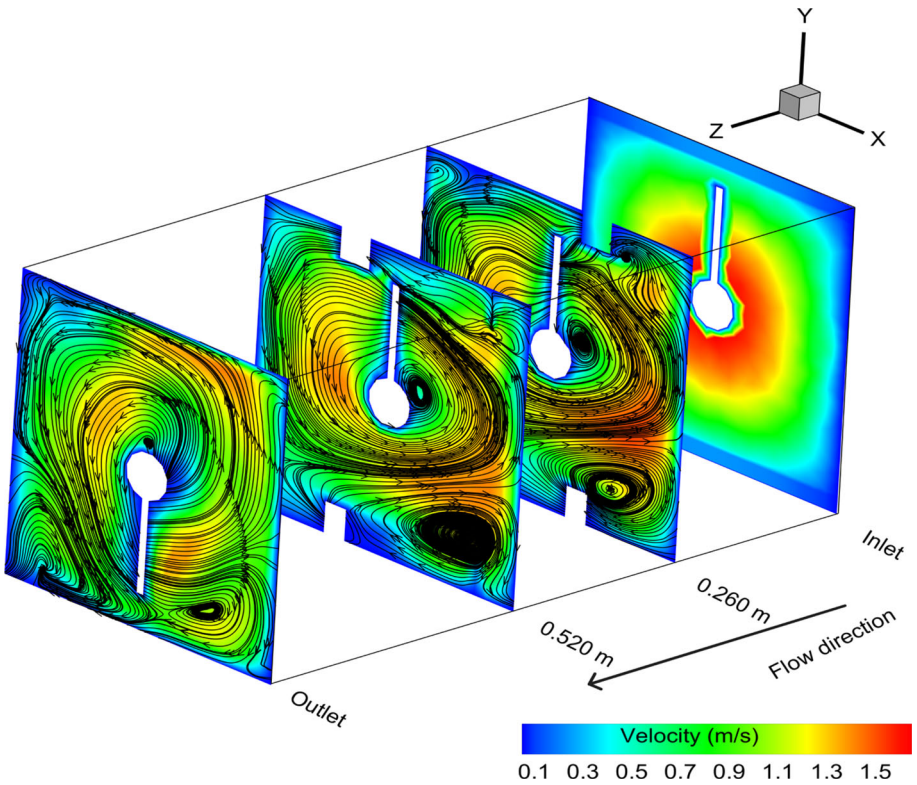

Fig. 16 Streamlines and velocity contours in a square duct fitted with 45° angled ribs on two opposite walls and HST, working fluid EG at Re = 750

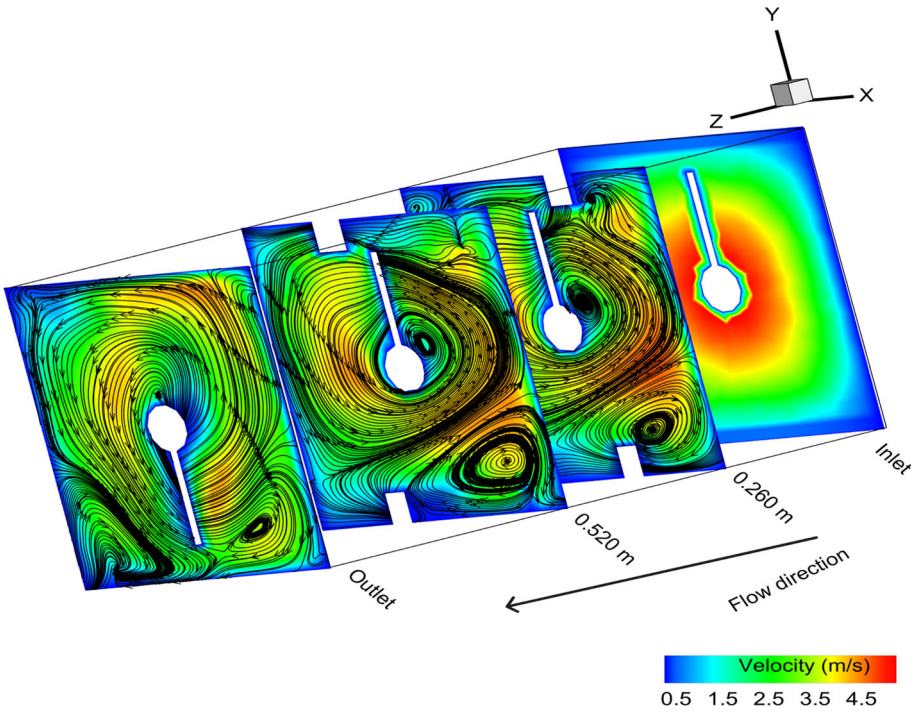

Fig. 17 Streamlines and velocity contours in a square duct fitted with 45° angled ribs on two opposite walls and HST, working fluid servo-therm oil at Re = 750

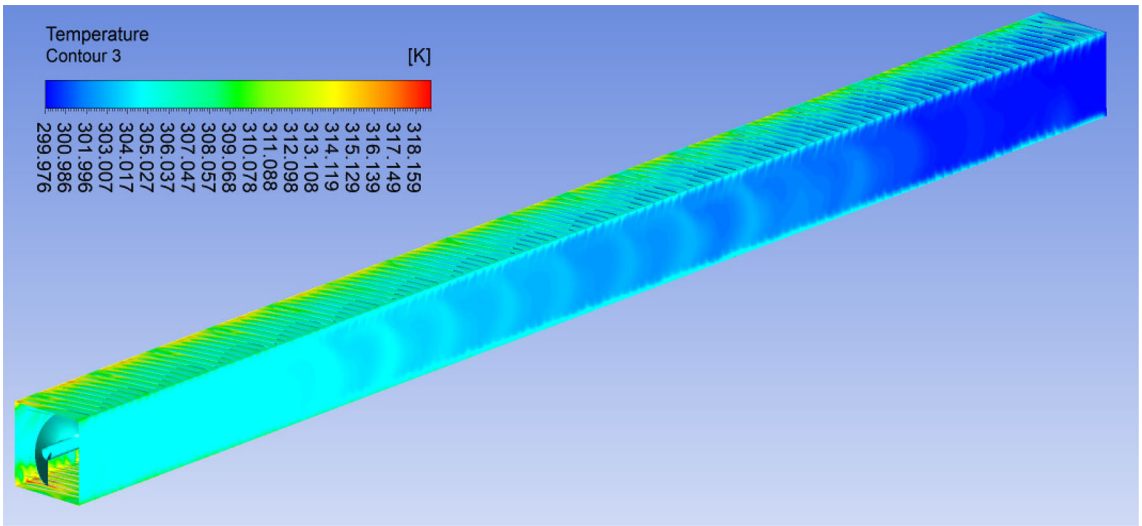

Fig. 18 Temperature distribution of water at Re = 500

ribs, three different rib angles are used to show the distinctive effect of ribs angle on heat transfer rate. The simulation results are revealing the fact that the performance of 45° angled ribs are better than that of 30°, 60° and 90° angled ribs. It should be noted that surface area is not changing. The foremost work of the angled ribs is to separate boundary layer and decrease the thermal resistance in the vicinity of the boundary surface. Out of different configuration, the 45° angled ribs from inlet is surpassing others. The 45° angled ribs in synergy with helical screw tape inserts are maneuvring the working fluids toward heated surface. The angled ribs are mixing the bulk fluid effectively and increasing the residence time. The above mentioned reasons support the heat transfer augmentation. The Nusselt number for different angled ribs in combination with HST at Reynolds number 200 is presented in Fig. 11. The Nusselt number corresponding to 45° angled ribs is the highest among all. The heat transfer enhancement techniques are not performing well below Reynolds number 200. Below Reynolds number 200, the velocity at the inlet is small and the swirling effect is not prominent at low velocity.

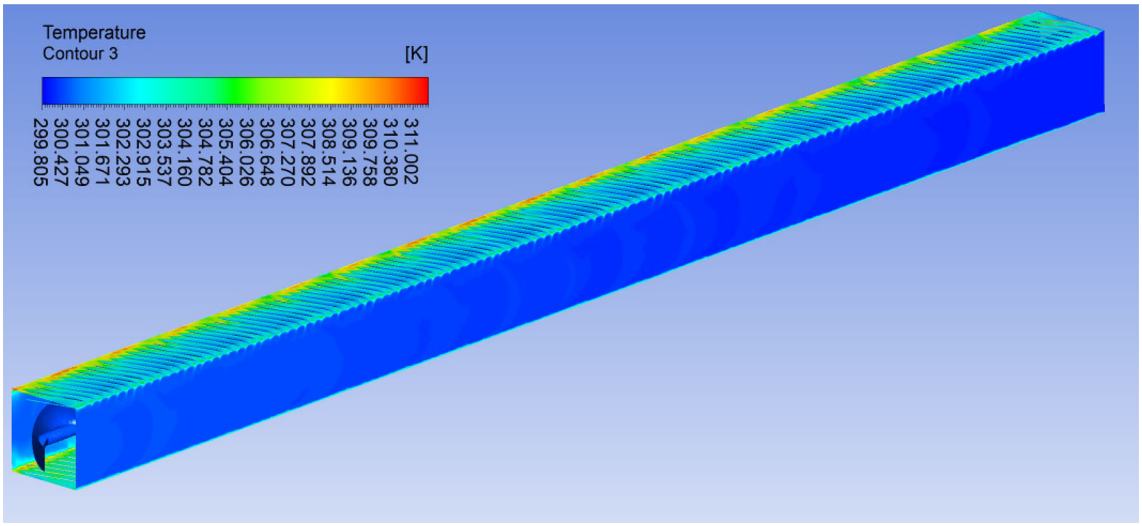

Fig. 19 Temperature distribution of ethylene glycol at Re = 500

Fig. 20 Temperature distribution of Servo-therm oil at Re = 500

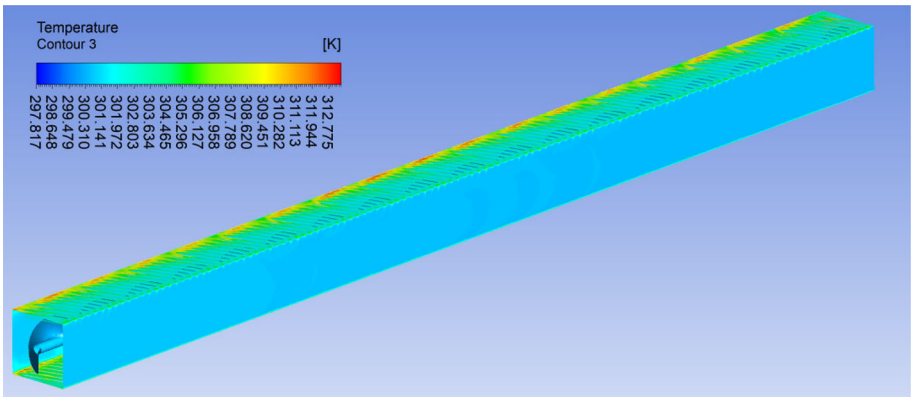

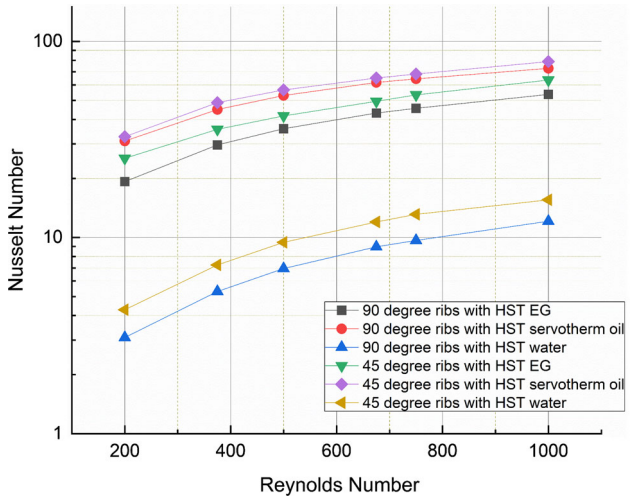

Fig. 21 Effect of rib angles (45° and 90°) on Nusselt number (helical screw tape insert is present in each case)

The combination of above-mentioned passive techniques act in different way with different working fluids. To visualize the combined effect of passive techniques on heat transfer rate, streamlines of different working fluids at a fixed Reynolds number is presented in the Figs. 12, 13 and 14. The streamlines are presented in *YZ*-plane. Additionally, the temperature profile is shown with streamlines too. In the case of water, there a number of eddies forming in the vicinity of ribs whereas the eddies vanish with working fluids Ethylene glycol and Servo-therm oil. This is happening due to viscosity difference between water and Servo-therm oil. The eddies increases the residence time and promote the bulk mixing. Thus, in Fig. 12, the bulk temperature reached around 305 K whereas for viscous fluids (Ethylene Glycol and Servo-therm oil), the bulk temperature is nearly about the inlet temperature and has been represented in Figs. 13 and 14.

Also, the velocity profile and the streamlines in *XY* plane is essential to understanding the mechanism of heat transfer. In all the cases, the working fluid is rotating around the core rod, and directed toward the outer face. At the inlet section, a fully developed velocity profile has been introduced. This signifies that the maximum value of velocity should be at the center but due to the positioning of the core rod and helical

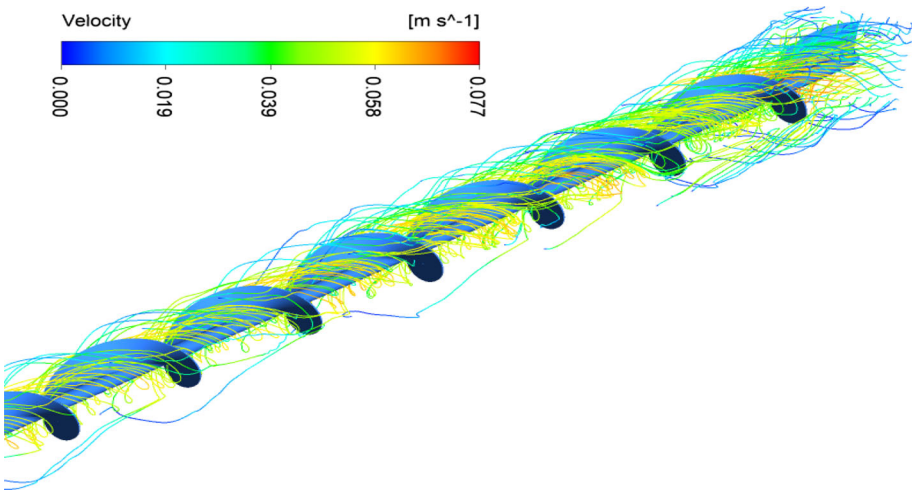

Fig. 22 Streamlines of water at Reynolds number 500

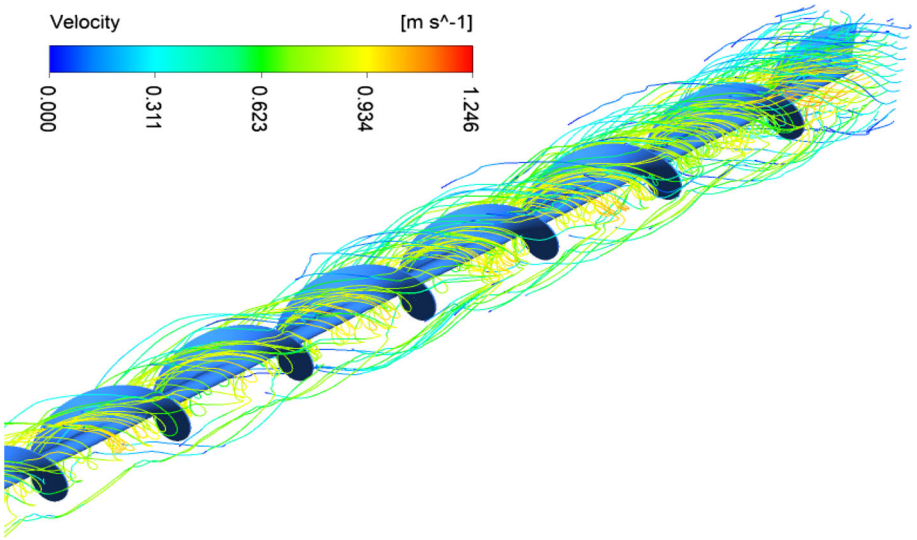

Fig. 23 Streamlines of ethylene glycol at Reynolds number 500

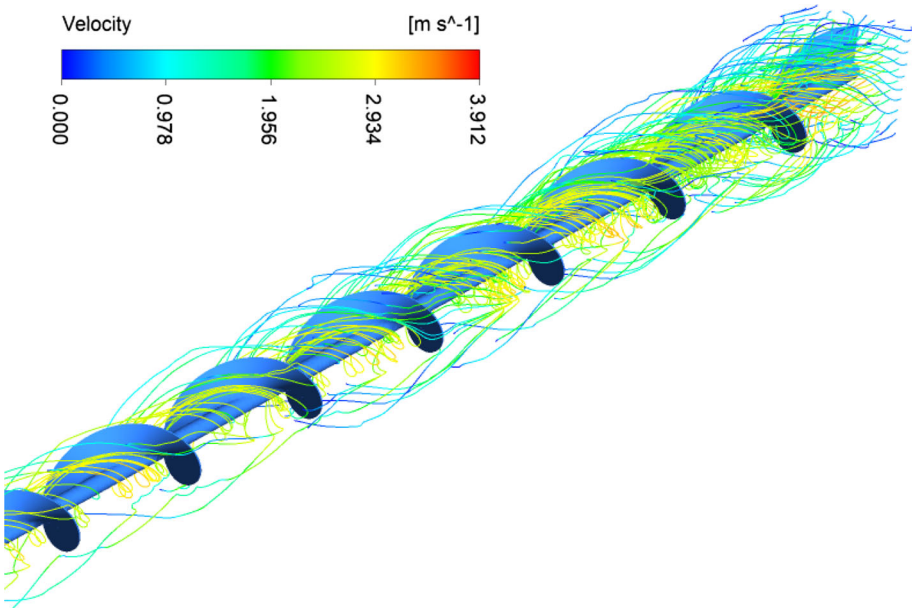

Fig. 24 Streamlines of servo-therm oil at Reynolds number 500

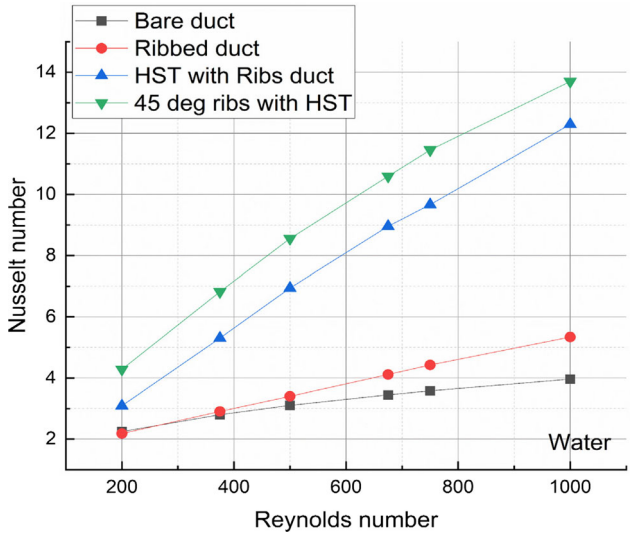

Fig. 25 Comparison between bare duct, ribbed duct, HST with transverse ribs and HST with 45° angled ribbed duct for water

fins, the velocity is maximum between the outer wall and the central core rod. The velocity profile with streamlines for three working fluids has been presented in Figs. 15, 16, and 17. The figure reveals that the proper mixing is occurring because at the inlet position, the maximum velocity is concentrated near the core rod. At positions 0.260 m, 0.520 and at the outlet, the velocity is not concentrated near the core rod. The formation of eddies is visible too.

The full length model and their temperature distribution throughout the length for working fluids water, EG and Servo-therm oil have been represented in Figs. 18, 19, and 20 respectively. The two sides fitted with ribs are enhancing the heat transfer rate. The remaining sides being affected by the ribbed wall too. The temperature scale is on higher side with the working fluid water because the specific heat capacity of water is higher than the Servo-therm oil and Ethylene Glycol. The temperature scale of the EG and Servo-therm oil is almost same because there is not difference between their specific heat. The temperature profile is generated at Reynolds number 500.

The above-mentioned combination of techniques is properly mixing water whereas the effectiveness of compound heat transfer enhancement techniques reduces with viscous fluid (EG and Servotherm oil). The Servo-therm oil and EG can produce high heat transfer at high Reynolds number because more flux will enter and leave the control volume in a fixed time.

The Nusselt number is increasing with the increase in Reynolds number because the convective heat transfer rate increases with an increase in velocity. The viscosity of Servo-therm oil is higher than the other two and inserts are present in the duct. The duct fitted with inserts are having high surface area than the bare duct. Thus, viscous fluid is sticking to the wall surface more than the less viscous fluids, and so the thermal resistances are higher in viscous fluids. Thus, the same heat transfer enhancement combination will act more effectively for high Reynolds number when the working fluid is Servo-therm oil and EG. It should be noted that the heat flux is applied on the two opposite faces only.

The increase in Nusselt number is due to the combination of passive techniques. The comparison of the Nusselt number for 45-degre angled ribs and the transverse ribs is presented in Fig. 21. The helical screw tape inserts are present in both conditions. The Nusselt number corresponding to working fluid servo-therm oil and 45° angle ribs with HST is the highest among all. The helical screw tape inserts are generating the swirls. This increases the bulk mixing of the fluid whereas angled ribs decrease the thickness of the boundary layer. Bulk mixing means fluid will not flow in layers as typically occurs in the laminar flow regime. Also, the residence time increases as a large number of fluid particles come in direct contact with the heated surface. The boundary layer thermal resistance is higher due to boundary layer formation. The boundary layers are taken care of by ribs. The ribs act as obstacles and the fluid particles following a straight line hit the ribs and change direction. The temperature gradient is more prominent after helical fins. Although, there is an increase in pressure drop but boundary layer thermal resistance decreases significantly. Also, the swirling effect is helping in reducing the boundary layer thermal resistance.

The 3D streamlines over the helical screw tape insert with core rod are shown in Figs. 22, 23 and 24. The effect of helical screw tape insert is producing swirls and the bulk fluid is mixing with the fluids near the vicinity of heated wall. The peripheral streamlines are converging toward the center and some of streamlines has been vanished because of ribs. Although, there is not a significant change in streamlines for different working fluids, still the figures reveal that fluid is rotating around the core rod.

The Nusselt number depends on the Reynolds number and Prandtl number. The introduction of transverse ribs and helical screw tape inserts is disturbing the flow. However, at low Reynolds number, the periodic ribs are not performing well. The shape factor H plays an important role. The boundary layers separate due to the introduction of blunt bodies. In this research, the ribs are reducing the thickness of the boundary layer and thermal resistance. It should be noted that the maximum local heat transfer coefficient is at the reattachment point. The more the reattachment point, the more the heat transfer augmentation. Thus, ribbed wall duct performance is better than the bare duct. The Nusselt number versus Reynolds number for water has been shown in Fig. 25.

The combination is better than that of ribbed and bare ducts. The heat transfer augmentation depends on the mainstream fluid viscosity and the fluid viscosity near the wall. The helical screw tape reduces the velocity gradient which

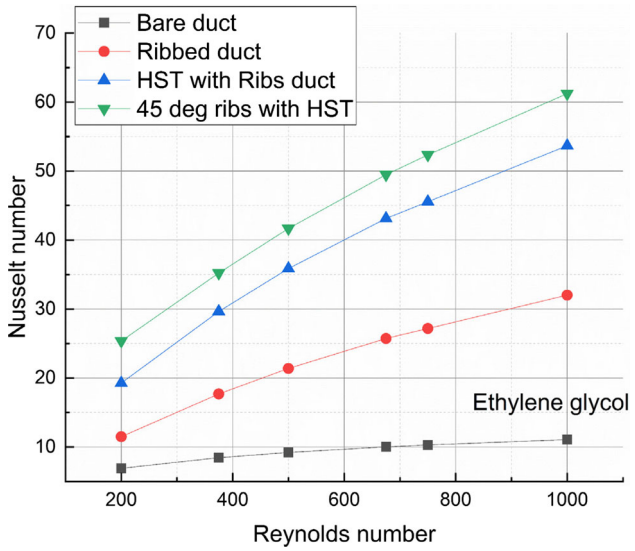

Fig. 26 Comparison between bare duct, ribbed duct, HST with transverse ribs and HST with 45° angled ribbed duct for EG

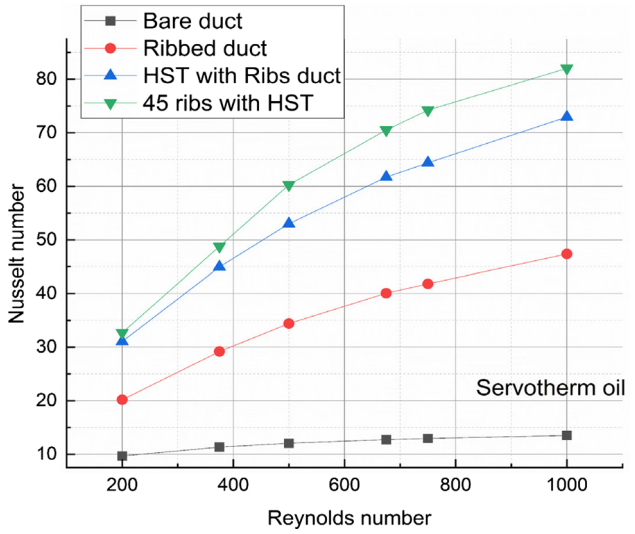

Fig. 27 Comparison between bare duct, ribbed duct, HST with transverse ribs and HST with 45° angled ribbed duct for servo-therm oil

is always present in the laminar flow regime. The viscosity of Servo-therm oil is higher than the other two working fluids, so, the heat transfer augmentation of Servo-therm oil is best among all. Figures 26 and 27 show the effect of heat transfer augmentation techniques on Ethylene glycol and Servo-therm oil under uniform wall heat flux condition. The 45° angled ribs with HST performance is better in each condition.

The passive heat transfer enhancement techniques increase the friction factor too. Thus, performance evaluation is essential in this case. Here, we are using "Thermal Enhancement Factor". The TEF for all three working fluids

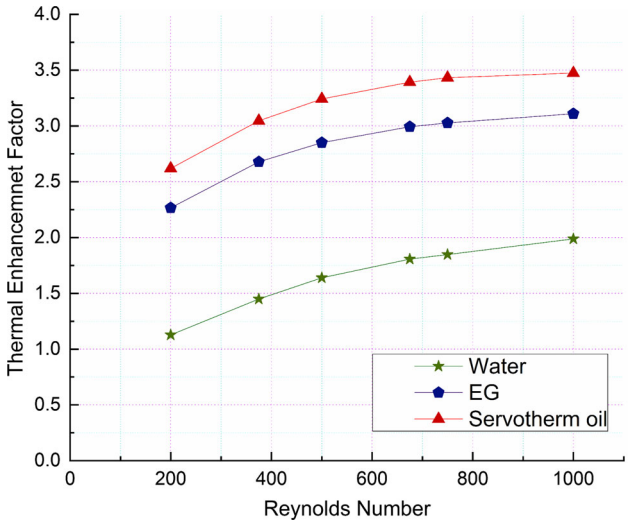

Fig. 28 TEF for water, ethylene glycol and servo-therm oil

are presented in the Fig. 28. The Servo-therm oil is performing extremely good because of better mixing. The above results are showing that the Servo-therm oil with transverse ribs and helical screw tape inserts should be used in the square duct. The combination will increase performance up to many folds under uniform wall heat flux applied on two opposite faces only.

8 Conclusions

- The Nusselt number is increasing with an increase in the Reynolds number for the three working fluids for each considered case.
- At Reynolds number 200, the Nusselt number achieved by 45° angled ribs with HST is 4.3% higher than the 30° angled ribs with HST, 22.26% higher than the 60° angled ribs, and 35.82% higher than the transverse ribs with HST.
- The combination increases the heat transfer rate. The heat transfer rate due to the combination of passive techniques is greater than the bare duct and ribbed duct.
- The reason for heat transfer enhancement is the bulk mixing of working fluid due to helical screw tape and increases in local heat transfer rate due to periodic transverse and angled ribs. The "Thermal Enhancement Factor" is greater than 1 for all cases.
- The performance of Ethylene Glycol is between the two other fluids because the viscosity of Ethylene Glycol lies between the viscosity of Servo-therm oil and Water. Servo-therm oil viscosity is the highest of all working fluids.
- In future, the above-mentioned configuration can be used for turbulent flow because it reduces boundary layer thickness effectively (Generation of eddies) and could be advantageous for industries.

- In future, the effect of different rib materials and working fluids on heat transfer characteristics can give a new dimension to the present study.

Acknowledgements I like to thank IIEST Shibpur and the Ministry of Education, Government of India.

Declarations

Conflict of interest All authors declare that they have no conflict of interest.

References

1. Incropera, F.P.; Lavine, A.S.; Bergman, T.L.; DeWitt, D.P.: Fundamentals of Heat and Mass Transfer. Wiley (2007)
2. Shah, R.K.; Sekulic, D.P.: Heat exchangers. Handb. Heat Transf. 3 (1998).
3. Ahmed, M.S.; Abedin, M.Z.: Review on heat transfer enhancement by insert devices. Int. J. Eng. Mater. Manuf. **5**(4), 130–147 (2020)
4. Deshmukh, P.W.; Kasar, S.V.; Prabhu, S.V.: A comprehensive compendium on passive augmentation techniques for enhancement of single-phase heat transfer coefficients in heat exchanger tubes under laminar and turbulent flow conditions. Heat Transf. Eng. **44**(6), 530–579 (2023)
5. Patil, S.V.; Babu, P.V.V.: Heat transfer augmentation in a circular tube and squareduct fitted with swirl flow generators: a review. Int. J. Chem. Eng. Appl. **2**(5), 326 (2011)
6. Sivashanmugam, P.; Suresh, S.: Experimental studies on heat transfer and friction factor characteristics of turbulent flow through a circular tube fitted with regularly spaced helical screw-tape inserts. Appl. Therm. Eng. **27**(8–9), 1311–1319 (2007)
7. Rout, P.K.; Saha, S.K.: Laminar flow heat transfer and pressure drop in a circular tube having wire-coil and helical screw-tape inserts. J. Heat Transf. (2013). https://doi.org/10.1115/1.4007415
8. Ranjan, H.; Bharti, A.K.; Emani, M.S.; Meyer, J.P.; Saha, S.K.: New combined heat transfer enhancement techniques used in laminar flow through non-circular ducts. Appl. Therm. Eng. (2019). https://doi.org/10.1016/j.applthermaleng.2019.114325
9. Chaurasia, S.R.; Sarviya, R.M.: Experimental analysis on thermal and friction factor characteristics of fluid flow in tube with novel double strip helical screw tape. Proc. Inst. Mech. Eng. Part A J. Power Energy **234**(6), 874–886 (2020)
10. Ranjan, H.; Saha, S.K.: Hydro-thermal characteristics of laminar flow through a square duct having transverse ribs and helical screw-tape inserts. Int. Commun. Heat Mass Transf. **130**, 105823 (2022)
11. Han, J.C.; Park, J.S.: Developing heat transfer in rectangular channels with rib turbulators. Int. J. Heat Mass Transf. **31**(1), 183–195 (1988). https://doi.org/10.1016/0017-9310(88)90235-9
12. Promvonge, P.; Sripattanapipat, S.; Tamna, S.; Kwankaomeng, S.; Thianpong, C.: Numerical investigation of laminar heat transfer in a square channel with 45 inclined baffles. Int. Commun. Heat Mass Transf. **37**(2), 170–177 (2010)
13. Saha, S.K.; Swain, B.N.; Dayanidhi, G.L.: Friction and thermal characteristics of laminar flow of viscous oil through a circular tube having axial corrugations and fitted with helical screw-tape inserts. J. Fluids Eng. Trans. ASME **134**(5), 1–9 (2012). https://doi.org/10.1115/1.4006669
14. Saha, S.; Saha, S.K.: Enhancement of heat transfer of laminar flow through a circular tube having integral helical rib roughness and fitted with wavy strip inserts. Exp. Therm. Fluid Sci. **50**(3), 107–113 (2013). https://doi.org/10.1016/j.expthermflusci.2013.05.010
15. Moon, M.-A.; Park, M.-J.; Kim, K.-Y.: Evaluation of heat transfer performances of various rib shapes. Int. J. Heat Mass Transf. **71**, 275–284 (2014)
16. Keklikcioglu, O.; Ozceyhan, V.: A review of heat transfer enhancement methods using coiled wire and twisted tape inserts. Heat Transf. Methods Appl. (2018).
17. Sharma, N.; Tariq, A.; Mishra, M.: Experimental investigation of heat transfer enhancement in rectangular duct with pentagonal ribs. Heat Transf. Eng. **40**(1–2), 147–165 (2019)
18. Ali, U.; Rehman, K.U.; Malik, M.Y.; Zehra, I.: Thermal aspects of Carreau fluid around a wedge. Case Stud. Therm. Eng. **12**(May), 462–469 (2018). https://doi.org/10.1016/j.csite.2018.06.006
19. Ali, U.; Rehman, K.U.; Alshomrani, A.S.; Malik, M.Y.: Thermal and concentration aspects in Carreau viscosity model via wedge. Case Stud. Therm. Eng. **12**(April), 126–133 (2018). https://doi.org/10.1016/j.csite.2018.04.007
20. Rehman, K.U.; Alshomrani, A.S.; Malik, M.Y.: Carreau fluid flow in a thermally stratified medium with heat generation/absorption effects. Case Stud. Therm. Eng. **12**(March), 16–25 (2018). https://doi.org/10.1016/j.csite.2018.03.001
21. Rehman, K.U.; Al-Mdallal, Q.M.; Malik, M.Y.: Symmetry analysis on thermally magnetized fluid flow regime with heat source/sink. Case Stud. Therm. Eng. **14**(April), 100452 (2019). https://doi.org/10.1016/j.csite.2019.100452
22. Bibi, M.; Zeeshan, A.; Malik, M.Y.; Rehman, K.U.: Numerical investigation of the unsteady solid-particle flow of a tangent hyperbolic fluid with variable thermal conductivity and convective boundary. Eur. Phys. J. Plus (2019). https://doi.org/10.1140/epjp/i2019-12651-9
23. Acharya, N.; Öztop, H.F.: On the entropy analysis and hydrothermal behavior of buoyancy-driven magnetized hybrid nanofluid flow within a semi-circular chamber fitted with a triangular heater: application to thermal energy storage for energy management. Numer. Heat Transf. Part A Appl. 1–31 (2023).
24. Acharya, N.: Hydrothermal scenario of buoyancy-driven magnetized multi-walled carbon nanotube-Fe_3O_4-water hybrid nanofluid flow within a discretely heated circular chamber fitted with fins. J. Magn. Magn. Mater. **589**, 171612 (2024)
25. Eymard, R.; Gallouët, T.; Herbin, R.: Finite volume methods. In: Solution of Equation in $\mathbb{R}n$ (Part 3), Techniques of Scientific Computing (Part 3), vol. 7, pp. 713–1018. Elsevier (2000). https://doi.org/10.1016/S1570-8659(00)07005-8
26. Franks, F.: Water: A Matrix of Life, vol. 21. Royal Society of Chemistry (2000)
27. Taylor, C.A.; Rinkenbach, W.H.: Ethylene glycol. Ind. Eng. Chem. **18**(7), 676–678 (1926)

28. Uttarwar, S.B.; Raja Rao, M.: Augmentation of laminar flow heat transfer in tubes by means of wire coil inserts. J. Heat Transf. **107**(4), 930–935 (1985). https://doi.org/10.1115/1.3247523
29. Anderson, J.D.; Wendt, J.: Computational fluid dynamics, Vol. 206. Springer (1995)
30. Delplace, F.: Laminar flow of Newtonian liquids in ducts of rectangular cross-section a model for both physics and mathematics. Open Access J. Math. Theor. Phys. **1**(5), 198–201 (2018). https://doi.org/10.15406/oajmtp.2018.01.00034
31. Matsson, J.: An Introduction to ANSYS Fluent 2020. SDC Publications (2020)
32. Patankar, S.V.; Spalding, D.B.: A calculation procedure for heat, mass and momentum transfer in three-dimensional parabolic flows. In: Numerical Prediction of Flow, Heat Transfer, Turbulence and Combustion, pp. 54–73. Elsevier (1983)
33. Kays, W.M.; Crawford, M.E.; Weigand, B.: Convective Heat and Mass Transfer: Tata McGraw-Hill Education. McGraw-Hill Education, Boston (2012)
34. Kline, S.J.: The purposes of uncertainty analysis. J. Fluids Eng. Trans. ASME **107**(2), 153–160 (1985). https://doi.org/10.1115/1.3242449
35. Saha, S.K.; Ranjan, H.; Emani, M.S.; Bharti, A.K.: PEC for two-phase flow (2020). https://doi.org/10.1007/978-3-030-20758-8_4